Classical conditioning drives learned reward prediction signals in climbing fibers across the lateral cerebellum

William Heffley and Court Hull*

Department of Neurobiology, Duke University School of Medicine, Durham NC, United States

*Correspondence: Court Hull

Email: Hull@neuro.duke.edu

Abstract

Classical models of cerebellar learning posit that climbing fibers operate according to a supervised learning rule to instruct changes in motor output by signaling the occurrence of movement errors. However, cerebellar output is also associated with non-motor behaviors, and recently with modulating reward association pathways in the VTA. To test how the cerebellum processes reward related signals in the same type of classical conditioning behavior typically studied to evaluate reward processing in the VTA and striatum, we have used calcium imaging to visualize instructional signals carried by climbing fibers across the lateral cerebellum before and after learning. We find distinct climbing fiber responses in three lateral cerebellar regions that can each signal reward prediction. These instructional signals are well suited to guide cerebellar learning based on reward expectation and enable a cerebellar contribution to reward driven behaviors, thus suggesting a broad role for the lateral cerebellum in reward-based learning.

Introduction

The cerebellum plays a key role in motor control and motor learning. However, it is becoming widely appreciated that the cerebellum also contributes significantly to many non-motor processes (Schmahmann, 1991) such as cognition (Kim et al., 1994), social processing (Van Overwalle et al., 2014), aggression (Reis et al., 1973) and emotion (Schmahmann and Caplan, 2006). Moreover, cerebellar deficits are associated with non-motor conditions including autism spectrum disorders (Wang et al., 2014), deficits of language processing and vocal learning (Ackermann, 2008), schizophrenia (Mothersill et al., 2016) and other impairments (Ivry and Spencer, 2004). Together, these observations strongly suggest that the cerebellum, and cerebellar learning, must operate in a manner compatible with adjusting motor as well as non-motor processes.

Classical models posit that cerebellar learning is instructed by signals carried by an afferent fiber projection from the inferior olive called climbing fibers (Albus, 1971; Ito, 1972; Marr, 1969). Such models suggest that climbing fibers operate according to a supervised learning rule to instruct changes in motor output by signaling the occurrence of movement errors. However, it is unclear how such a supervised learning rule could contribute to modification of many non-motor behaviors. In line with this view, accumulating evidence has demonstrated a wide range of climbing fiber responses that are distinct from motor error signals (Kitazawa et al., 1998; Streng et al., 2017), including prediction error and reward related signals (Heffley et al., 2018; Kostadinov et al., 2019; Larry et al., 2019; Ohmae and Medina, 2015). Together, such data provide evidence

that the cerebellum may utilize alternative learning rules to support a wider range of behaviors than can be driven by error-based supervised learning alone.

Under what conditions might the climbing fiber system instruct alternative learning rules? Rabies tracing experiments have identified a disynaptic pathway from the lateral cerebellum to the striatum (Hoshi et al., 2005), and recent functional connectivity experiments have revealed a direct, monosynaptic connection from the lateral cerebellum to the ventral tegmental area (VTA) (Carta et al., 2019). These experiments also showed that lateral cerebellar output can modulate reward-driven behaviors by the same pathway. If the cerebellum acts to modulate striatal and VTA pathways involved in reward-driven behaviors, it must contain information related to such behaviors, and likely mediate cerebellar learning in a manner consistent with reward-based associations. Indeed, there is evidence that cerebellar granule cells can display reward related signals (Wagner et al., 2017), and climbing fibers can display signals consistent with reward prediction errors in certain behaviors (Heffley et al., 2018; Ohmae and Medina, 2015). However, it remains unclear how cerebellar learning, and in particular, how learning signals provided by cerebellar climbing fibers, operate during the types of classical conditioning behaviors classically studied to evaluate reward processing and learning in the VTA and striatum.

A key first step in understanding how cerebellar learning can contribute to reward processing and reward driven behaviors is to test what instructional signals are carried by cerebellar climbing fibers in behavioral paradigms known to involve striatal computations. To this end, we have utilized an appetitive classical conditioning task that mirrors well-studied reward prediction paradigms (Schultz et al., 1997), and performed *in vivo* calcium imaging to measure cerebellar climbing fiber driven complex spike (Cspk) activity across the lateral cerebellum in awake mice. These experiments reveal distinct, functionally compartmentalized, reward-related Cspk signals in each of the lateral cerebellar lobules. Specifically, in Lobule Simplex (LS), Crus I and Crus II, robust Cspk responses emerge with learning in response to a visual cue that predicts reward. In LS and Crus II, unexpected reward produces Cspk responses, both before and after learning. In contrast, Crus I shows no Cspk response to unexpected reward in naïve animals, but a robust Cspk response to unexpected reward once animals have associated a visual cue with reward. Imaging Cspk activity across learning suggests that the same climbing fibers that respond to reward in naïve animals can instead respond to a reward predictive cue after learning. Finally, we observe no evidence of negative prediction error following reward omission immediately after learning, suggesting the possibility that Cspk responses may not instruct a strict temporal difference (TD) learning model in this paradigm. The learned, reward predictive Cspk signals

observed here are, however, consistent with a model that would allow learned cerebellar output to provide information about rewarding stimuli to downstream structures such as the VTA and striatum. Hence, these data provide a key link between the instructional signals known to be involved in cerebellar learning and the types of reward-based processing observed in downstream areas.

Results

An appetitive classical conditioning paradigm to investigate climbing fiber responses in the lateral cerebellum

To investigate climbing fiber driven Cspk activity during an appetitive classical conditioning paradigm that parallels tasks typically used to study reward processing in the VTA and striatum, we first established an appropriate behavior for head-fixed mice that is compatible with calcium imaging in the lateral cerebellum (**Fig 1A-D**). In this task, mice learn a simple association between a visual cue and the timing of subsequent reward delivery. Specifically, mice were trained by viewing a continuously present, full screen vertical grating that was transiently (100 ms) replaced with a horizontal grating to signal the delivery of a saccharine reward at a 600 ms delay (**Fig 1D**). After multiple training sessions (mean = 5.7 ± 0.4 days), mice learned the association between the visual cue and the time of reward delivery, significantly reducing both their reaction times (Day 1, 742.8 ± 25.4 ms; Day N+1, 544.7 ± 13.0 ms; $p=8.52\times10^{-8}$, n = 27 mice, paired t-test, **Fig. 1 E**) and miss rates (Day 1, 0.39 ±0.04; Day N+1, 0.03 ±0.01; $p=6.37\times10^{-9}$, paired t-test, **Fig. 1 F**). In addition to developing well-timed licking responses that approximated the time of reward delivery on rewarded trials, mice also developed robust licking responses following the visual cue on omission trials after learning that were absent in naïve animals (**Fig. 1G**). Together, these data indicate that mice successfully learn the association between visual cue and the timing of reward delivery in this paradigm.

Cspk activity shifts earlier in time after learning

We began by measuring Cspk activity before and after learning in lobule simplex (LS), where previous work has identified reward-related activity in granule cells and climbing fibers after learning in different behavioral paradigms (Heffley et al., 2018; Kostadinov et al., 2019; Wagner et al., 2017). To obtain a broad view of Cspk activity across LS and assess whether any reward-related signals are carried by climbing fibers in this paradigm, we first performed single-photon, mesoscale calcium imaging of Purkinje cell (PC) dendrites expressing GCaMP6f (**Fig. 2A**). This

method has previously been demonstrated to accurately report Cspk activity (Heffley et al., 2018). Using this approach, we observed a significant increase in the Cspk activity following reward delivery in naïve animals (n = 308 trials, 5 mice, p =5x10^{-19}, paired t-test), but no significant response on reward omission trials (n =74 trials, 5 mice, p =0.595, paired t-test) (**Fig. 2B, top**). After learning, significant Cspk responses were maintained (n =749 trials, 6 mice, p = 3.3 x10^{-100}, paired t-test), but were shifted in time, and preceded reward delivery on rewarded trials (**Fig. 2B, bottom, Fig. 2C**). Moreover, after learning there was also a significant response on omission trials preceding reward delivery (n =156 trials, 6 mice, p = 5.4 x 10^{-16}, paired t-test) (**Fig. 2B, bottom, Fig. 2D**). Across experiments, the latency of Cspk activity decreased significantly (n = 6 mice, p=1.04×10^{-6}, paired t-test) (**Fig. 2C**). Notably, this shift in Cspk timing (Δ_{Cspk} = 441 ms) was greater than the change in lick timing (Δ_{lick} = 185 ms), indicating that the Cspk response did not simply follow the timing of motor output. In addition, we find that Cspk responses after learning had the same timing for rewarded and omission trials (Rewarded trial latency = 383 ±15 ms, Omission trial latency = 378 ±19ms, n =6 mice, p=0.78×10^{-6}, paired t test) (**Fig. 2D**). In contrast, when reward was delivered unexpectedly after learning (i.e. in absence of the visual cue), Cspk activity followed reward delivery, and was significantly delayed compared with rewarded trials (Day N+2; rewarded trial latency = 366.1 ±31 ms, unexpected trial latency 793 ± 31ms, n = 5 mice, p=2.40×10^{-4}, paired t-test). The latency of Cspk responses on unexpected reward trials was, however, equivalent to the timing of responses to rewarded trials in naïve animals (p=0.38, two-sample t-test) (**Fig. 2E**). Together, these data reveal that complex spiking shifts in time as a result of learning, initially following reward delivery in naïve animals and later preceding reward delivery in trained animals, occurring with the same timing on both rewarded an omission trials after learning.

Cspk responses in LS signal reward predictions that emerge with learning

Our mesoscale imaging experiments suggest that Cspk activity in LS exhibits reward-related activity that changes as a function of learning in manner that is consistent with reward expectation. However, to further disambiguate Cspk activity related to reward, reward expectation and licking, and to test whether Cspk activity in individual PC dendrites changes across learning, we next used two-photon imaging to visualize Cspk responses in individual PC dendrites. As in our mesoscale imaging experiments, these data revealed significantly elevated Cspk rates following reward delivery in naïve animals (n = 1040 dendrites, 15 mice, p = 5.5 x 10^{-48}, one-tailed t-test) (**Fig. 3A,D, Supplement 1**) but no significant response during this window on omission trials (p = 0.98). After learning, we observed significantly elevated Cspk rates prior to reward delivery on

both rewarded (n = 906 dendrites, 16 mice, $p = 2.3 \times 10^{-60}$, one-tailed t-test) and omission trials ($p = 1.4 \times 10^{-33}$) that were comparable across trial types (p = 0.01, paired t-test; **Fig. 3B,C,E**). In addition, post-reward Cspk rates were significantly reduced after learning ($p = 2.0 \times 10^{-19}$, unpaired t-test), with small elevations in spiking (reward trials: $p = 3.3 \times 10^{-4}$; omission trials: $p = 6.7 \times 10^{-6}$; one-tailed t-test) that were equivalent on both rewarded and omission trials (p = 0.46; paired t-test). Notably, there were no Cspk responses that were reliably suppressed below baseline after the time of expected reward on omission trials (see Methods). These data indicate that Cspk activity shifts from an association with reward prior to learning to the cue that predicts reward after learning. To test whether unique populations of PC dendrites exhibit Cspk responses to reward and following the visual cue after learning, we identified the subset of PC dendrites with significant post-reward responses (n = 204/906 dendrites; **Fig. 3 – Figure Supplement 2**). This small subset of PC dendrites also responded following the visual cue ($p = 5.9 \times 10^{-36}$; one-tailed t-test), indicating that a minority of PC dendrites can exhibit Cspk responses to both reward and the visual cue after learning. These data suggest the possibility that some Cspk responses had not fully transitioned between encoding the reward and the reward-predicting cue immediately after learning. However, the majority of PC dendrites (n = 702/906 dendrites) did not respond to the reward after learning, and instead only responded to the reward-predicting cue ($p = 3.9 \times 10^{-36}$, one-tailed t-test; **Fig. 3– Figure Supplement 2**).

To disambiguate Cspk responses related to reward versus reward expectation, we measured responses to unexpected reward after learning (Day N+2). On these trials, Cspk rates increased significantly after the time of unexpected reward delivery (n = 243 dendrites; 6 mice, $p = 1.6 \times 10^{-8}$, one-tailed t-test; **Fig. 3F**). Moreover, with this additional day of training, there was no longer a significant post-reward response on trials where reward was expected (p=0.8). These data indicate that after learning, Cspk responses in area LS are only reward responsive if the reward is unexpected. In the same experiments, Cspk rates increased significantly prior to reward delivery when reward was expected ($p = 1.2 \times 10^{-12}$, one-tailed t-test; **Fig. 3 F**). Notably, the PC dendrites that were significantly responsive following the reward-predicting cue (n = 84/243 dendrites), were also significantly responsive after the unexpected reward ($p = 2.3 \times 10^{12}$, one-tailed t-test; **Fig. 3G**). This suggests that the same PC dendrites exhibit Cspk responses to the reward-predictive cue and unexpected reward, thus signaling predictions under two different conditions. However, lick timing also differs between these two trial types, and changes across learning. Thus, we also sought to further disambiguate reward related Cspk responses from possible Cspk responses driven by motor output during licking.

To directly assess the role of licking in modulating Cspk rates, we first generated a lick-triggered average of Cspk activity from licks generated during the inter-trial interval (ITI). These data revealed no significant Cspk response to licking ($p = 0.6$; $n = 768$ dendrites, 13 mice, one-tailed t-test; **Fig. 3H**), consistent with previous reports showing a lack of lick-related Cspk activity in area LS (Bryant et al., 2010). To further address the contribution of licking to the emergent Cspk responses following the reward-predicting cue after learning, we segregated rewarded trials into subsets according to lick timing. Specifically, we averaged trials with the earliest and latest quartiles of licking. This analysis revealed that the peak of the pre-reward Cspks occurred at nearly the same time relative to the cue on trials with early as compared to late licks (Cspk latency on early trials: 300 ms; late trials: 330 ms), and with similar, but slightly smaller, amplitude ($p = 4.4 \times 10^{-4}$; $n = 906$ dendrites, 16 mice, paired t-test; **Fig 3I**). There was, however, a difference in Cspk rate following reward delivery ($p = 8.8 \times 10^{-9}$), likely due to the increased variability in the timing of reward consumption for trials with late licks. In addition, we also compared trials with the highest and lowest lick rates, and found that Cspk responses had identical timing (high and low lick rate Cspk latency = 300 ms; **Fig. 3J**) and a qualitatively similar, though statistically different amplitude prior to reward delivery ($p = 7.4 \times 10^{-05}$, paired t-test; **Fig. 3J**). These data indicate that the pre-reward Cspk responses that emerge with learning (**Fig. 3K,L**) are related to the cue driven expectation of reward, and not conditioned motor output due to licking.

The same climbing fibers can respond to reward and a reward-predictive visual cue

While our data indicate Cspk activity within individual dendrites can represent different reward-related events (i.e. the reward-predicting cue and unexpected reward), these data do not address whether it is the same climbing fibers that shift their responses, or whether separate populations of climbing fibers generate different responses before and after learning. To address this question, we measured Cspk activity from PC dendrites in the same coordinates before and after learning in a subset of experiments. To evaluate responses, we took two approaches. First, we manually identified individual PC dendrites across imaging days and measured their Cspk responses before and after learning (**Fig 4A,B**). This approach revealed clear examples of single PC dendrites with reward responsive Cspk activity in naïve animals that became cue responsive after learning. However, because this approach relies on user identification of the same PC dendrites, we also sought to test an automated approach. To do so, we first independently generated pixel masks for PC dendrites from our pre and post-learning fields of view (**Fig 4C-D**). We then motion registered the mean fluorescence image from the post-learning session to the

227 pre-learning session (**Fig 4E**), and applied the same pixel shifts from this registration to the
228 segmented pixel masks from the post-learning condition. By overlaying the shifted post-learning
229 pixel masks with the pre-learning masks, we assessed the overlap between imaging days (**Fig**
230 **4F-H**). Despite closely matched fields of view, this process led to a majority of PC dendrite masks
231 with little overlap. We thus employed a stringent criterion of greater than 50% overlap to increase
232 the probability of accurately identifying the same PC dendrites across imaging sessions. With
233 these criteria, we identified a group of PC dendrites likely corresponding to the same PC dendrites
234 before and after learning. In these PC dendrites, as in our other experiments, we find that Cspk
235 activity was initially absent following the visual cue in naïve animals ($p = 0.59$; $n = 61$ dendrites,
236 14 mice, one-tailed t-test; **Fig. 4I**), and that cue driven responses emerged with learning ($p =$
237 1.2×10^{-8}). We note that because of the close spacing and similar size and orientation of PC
238 dendrites, such approaches cannot provide definitive evidence of tracking the same PC dendrites
239 across learning. However, these data support the conclusion that individual CFs can develop a
240 learned response to the reward predictive cue as a result of learning (**Fig. 4J**).
241
242 **<u>Crus I and Crus II exhibit reward-related Cspk responses that are distinct from area LS</u>**
243 Anatomical and physiological evidence suggests that Cspk responses are functionally
244 compartmentalized across the medio-lateral axis of the cerebellum (Apps and Garwicz, 2005),
245 raising the possibility of different computations and diverse reward-related Cspk activity patterns
246 in lobules other than LS. Thus, we next measured Cspk responses in Crus I and Crus II .
247
248 In Crus I, pre-learning Cspk activity differed substantially from LS. Specifically, in naïve animals,
249 Cspk activity was sensory-related, and followed the visual cue at a time well before reward
250 delivery or licking on both rewarded ($p = 3.6 \times 10^{-20}$, $n = 133$ dendrites, 6 mice; one-tailed t-test;
251 **Fig. 5A,D**) and omission trials ($p = 3.4 \times 10^{-17}$). After learning, however, once the cue had been
252 associated with upcoming reward, Cspk responses to the visual cue were significantly enhanced
253 ($p = 2.3 \times 10^{-8}$, unpaired t-test, $n = 178$ dendrites, 7 mice; **Fig. 5B,C,E**). In contrast, there were
254 only weak or non-significant reward responses on rewarded or omission trials, either before
255 (rewarded: $p = 0.002$; omission: $p = 0.21$; one-tailed t-test; **Fig. 5D,E**) or after learning (rewarded:
256 $p = 1.0$; omission: $p = 0.84$; one-tailed t-test). Again, however, we did not identify any PC dendrites
257 that were reliably suppressed at the time of expected reward after learning. Notably, despite the
258 lack of a Cspk response to unexpected reward in naïve animals, there was a large Cspk response
259 to unexpected reward in the same animals after learning ($p = 5.1 \times 10^{-11}$, $n = 141$, 5 mice, one-
260 tailed t-test; **Fig. 5F**). These data suggest that in Crus I, where Cspk responses are sensory

261 related in naïve animals, activity can also be generated by expectations that are specifically linked
262 to a learned, reward-predictive sensory cue after learning.
263
264 To test whether the same PC dendrites that exhibit Cspk responses following the visual cue also
265 respond to unexpected reward, we identified those PC dendrites that were significantly cue
266 responsive. Indeed, these PC dendrites (n = 100/141) also showed a robust response to
267 unexpected reward ($p = 7.7 \times 10^{-11}$; one-tailed t-test; **Fig. 5G**), indicating that PC dendrites can
268 signal expectation under distinct conditions. As further evidence that Cspk responses in Crus I
269 are sensory related in naïve animals, there was no significant Cspk response to licks during the
270 ITI (p = 0.04; n = 93 dendrites, 4 mice, one-tailed t-test; **Fig 5E**). To test whether licking contributes
271 to the learned increase in response amplitude following the cue, we segregated trials according
272 to the timing of the first lick. This revealed that the timing (early and late lick Cspk latency: 230
273 ms) and amplitude (p = 0.04, paired t-test; **Fig 5I**) of Cspk activity following the visual cue was
274 largely independent of lick timing. In addition, we also compared trials with the highest and lowest
275 lick rates, and found the amount of licking also did not alter the timing (high and low lick rate Cspk
276 latency: 230 ms) or amplitude of pre-reward Cspk responses (p = 0.4, paired t-test; **Fig. 5J**). Thus,
277 as with lobule simplex, learned changes in Cspk responses are not related to conditioned motor
278 output due to licking. Together, these data indicate that Cspk activity in Crus I is sensory related
279 in naïve animals (**Fig. 5K**), but can also be modulated by reward expectation because it is
280 enhanced by associating the visual cue with reward (**Fig. 5E,L**), and driven by delivering a reward
281 unexpectedly (**Fig 5F**).
282
283 Finally, we measured Cspk activity in Crus II. Similar to area LS, Cspk rates were elevated in
284 response to reward delivery in naïve animals ($p = 2.7 \times 10^{-18}$; n = 147 dendrites, 5 mice, one-tailed
285 t-test; **Fig. 6A,D**), but not on reward omission trials (p = 1.0). After learning, a robust cue response
286 was observed in Crus II on both rewarded ($p = 9.7 \times 10^{-26}$; n = 245 dendrites, n=6 mice, one-tailed
287 t-test; **Fig. 6B,C,E**) and omission trials ($p = 6.1 \times 10^{-21}$). However, distinct from area LS, the
288 reward response persisted after learning ($p = 5.6 \times 10^{-11}$; **Fig. 6E**). Again, however, we observed
289 no significantly increased response on omission trials at the time of expected reward (p = 0.95);
290 nor did we observe any significant suppression. When reward was delivered unexpectedly after
291 learning, we observed enhanced Cspk rates as compared to the Cspk responses to expected
292 reward ($p = 1.1 \times 10^{-11}$, n = 184 dendrites, 6 mice; **Fig. 6F**), suggesting a component of the learned
293 response that scales with expectation. Notably, the same PC dendrites that respond to the cue

294 after learning (n = 60/184) continue to respond to both the expected ($p = 1.5 \times 10^{-4}$; one-tailed t-
295 test; **Fig. 6G**) and unexpected reward ($p = 1.1 \times 10^{-15}$) after learning.
296
297 In contrast with area LS and Crus I, in naïve animals we observed a significant lick related
298 response in Crus II as measured by the lick triggered average of Cspk activity during the ITI ($p =$
299 1.6×10^{-5}, n = 104; one-tailed t-test; **Fig. 6H**). This result is consistent with previous reports
300 suggesting that Cspk activity can be triggered by licking in this area (Gaffield et al., 2016; Gaffield
301 et al., 2018; Welsh et al., 1995). Interestingly, however, these responses disappeared after
302 learning (p = 0.98; n = 136 dendrites, 3 mice). Moreover, after learning, the pre-reward timing of
303 Cspks was independent of lick timing (Cspk latency on both early and late lick trials = 300 ms;
304 **Fig 6I**), and Cspks maintained a similar rate following the cue (p = 0.002; paired t-test; **Fig 6I**)
305 regardless of lick timing. In addition, we also compared trials with the highest and lowest lick
306 rates, and found the amount of licking also did not alter the timing of Cspk responses (high and
307 low lick rate Cspk latency = 300 ms; **Fig. 6J**), and produced Cspk responses with similar though
308 statistically different amplitude prior to reward ($p = 4.1 \times 10^{-5}$, paired t-test; **Fig. 6J**). These results
309 suggest that, while some activity can be driven by licking in naïve animals (**Fig. 6H**), motor output
310 alone is not the central determinant of Cspk activity in Crus II (**Fig. 6 H-L**).
311 Finally, we sought an additional approach to test whether movement contributes to the
312 cue-associated, post-learning Cspk responses in LS, Crus I and Crus II. While we have
313 demonstrated that Cspk responses do not correlate with licking, it remains possible that animals
314 exhibit additional conditioned responses that are uncorrelated with licking. We thus used a
315 piezoelectric sensor positioned under the animal to detect body movements during a subset of
316 our post-learning imaging sessions (**Fig. 7A**). This sensor is extremely sensitive to the smallest
317 movements, even registering the animals' breathing (**Fig. 7B**). Using this approach, we
318 segregated trials according to the most and least movement on trial-by-trial basis, and found no
319 relationship between the learned Cspk response and movement (High vs low movement Cspk
320 responses, LS: p = 0.13 , n= 316 dendrites, 5 mice; Crus I; p = 0.13 , n= 27 dendrites, 2 mice; p
321 = 0.10 , n= 97 dendrites, 3 mice; **Fig 7C-E**). These data strongly support the hypothesis that the
322 learned Cspk responses demonstrated here are driven by the reward-predictive visual cue, and
323 not reafference or sensory feedback related to movement.
324

325 **Discussion**

326 We have used a classical conditioning paradigm of the kind typically studied to evaluate reward
327 signaling in the VTA and striatum to reveal that climbing fibers provide a diverse set of learned

reward prediction signals across the lateral cerebellum. Specifically, in LS and Crus II, Cspk responses emerged as a function of learning to a cue that predicted upcoming reward. In Crus I, while a sensory-evoked Cspk response to the visual cue was already evident in naïve animals, this response was enhanced once the cue had been associated with upcoming reward. Hence, in all three areas, there was a learned Cspk response related to reward prediction. Cspk responses also exhibited significant differences across areas. In LS, the response to expected reward was largely lost after learning, but was pronounced when reward was delivered unexpectedly. In Crus I, while there was no reward response in naïve animals, a Cspk response to unexpected reward emerged only after the animals established an expectation of reward delivery in response to the visual cue. Finally, in Crus II, reward responses persisted across learning, even after a separate Cspk response emerged to the reward-predictive visual cue. The post-learning Cspk response to unexpected reward was enhanced, however, as compared to trials when reward was expected.

Together, these common, learned responses to a reward-predictive cue and to unexpected reward indicate that all three areas exhibit Cspk responses related to reward prediction. Such commonalities suggest a broad role for the lateral cerebellum in reward-based learning. The differences in responses, however, also suggest that learned changes in each area are overlaid on the unique sensory and motor Cspk signals pre-existing in each region. Thus, these data also indicate that the lateral cerebellum can harness other distinct sensory and motor signals across each area for different forms of sensorimotor learning, and perhaps to utilize alternate learning strategies that depend on task requirements.

Indeed, previous work supports the idea that LS, Crus I and Crus II may each have multiple functions, as they receive a diverse range of inputs, and have been implicated in both motor and non-motor behaviors. For example, climbing fibers in LS can carry somatosensory input related to forelimbs (Apps and Garwicz, 2005), but also exhibit responses consistent with reinforcement learning signals (Heffley et al., 2018; Kostadinov et al., 2019). Crus I climbing fibers can carry diverse sensory input related to visual, auditory and somatosensory stimuli (Gaffield et al., 2019; Ju et al., 2019), and Crus II climbing fibers can respond during various motor behaviors such as licking and whisker movement (Brown and Raman, 2018; Gaffield et al., 2016; Gaffield and Christie, 2017). Each of these areas also receives mossy fiber input that can convey both diverse sensory signals (Apps and Hawkes, 2009), as well as motor information (Brown and Raman, 2018; Chen et al., 2016, 2017). This combination of sensory and motor input has been suggested

362 to enable integration that allows the lateral cerebellum to modulate voluntary behaviors though
363 output to the neocortex (Proville et al., 2014). However, these lateral cerebellar regions have also
364 been implicated in non-motor behaviors (Badura et al., 2018; Carta et al., 2019; Deverett et al.,
365 2018; Schmahmann et al., 2019), and with cognitive deficits such as autism spectrum disorders
366 (Wang et al., 2014). Such contributions to cognitive processes may be enabled by connectivity
367 from these cerebellar regions to downstream targets such as the anterior cingulate cortex,
368 prefrontal cortex, orbitofrontal cortex (Badura et al., 2018), hippocampus (Hoshi et al., 2005;
369 McAfee et al., 2019) and striatum (Hoshi et al., 2005). In combination, this apparent complexity
370 of connectivity and function suggests that correlations between neural activity and discrete
371 behavioral parameters in absence of additional information about behavioral state or task goals
372 may be insufficient to infer how these regions contribute to behavior.
373
374 In this study, cue and reward-associated Cspk responses could be clearly distinguished from
375 motor responses due to licking or other movement in all three areas, as the timing or amount of
376 licking did not correlate with Cspk responses, nor did overall movement as measured piezoelectric
377 sensor. In a previous study, we identified a subset of lick-responsive PC dendrites after learning
378 in area LS, and we concluded that such Cspk responses were learned and related to reward
379 expectation rather than motor output per se (Heffley et al., 2018). Here, by imaging naïve animals,
380 we were able to demonstrate no significant lick response in absence of learning in area LS and
381 Crus I, consistent with previous reports indicating Cspk responses to licking are localized primarily
382 to Crus II (Gaffield et al., 2016; Gaffield et al., 2018; Welsh et al., 1995). Also in agreement with
383 these data, we did observe a significant Cspk response to licking in Crus II in naïve animals.
384 Interestingly, however, once the association between visual cue and reward had been
385 established, licking during the ITI when no reward was possible failed to produce Cspk activity.
386 These data suggest that even in areas with motor related signals, Cspk responses are more
387 complex than was previously appreciated. While earlier studies investigating Cspk responses to
388 licking did not attempt to disambiguate between motor output, reward, and reward expectation
389 (Bryant et al., 2010; Gaffield et al., 2016; Gaffield et al., 2018; Welsh et al., 1995), we suggest
390 that such efforts are crucial to understanding the role Cspk signals in cerebellar learning.
391
392 This study is part of a growing literature suggesting new roles for climbing fiber signals that are
393 distinct from classical error-based supervised learning (Heffley et al., 2018; Kitazawa et al., 1998;
394 Kostadinov et al., 2019; Ohmae and Medina, 2015; Streng et al., 2017). In a previous study, we
395 identified Cspk activity consistent with an unsigned reinforcement learning rule in an operant

396 conditioning task after learning (Heffley et al., 2018). In this study, we measured Cspk activity
397 both before and after learning in a task with different requirements, and found responses that
398 showed many similarities but also significant differences in Cspk activity. In both tasks, we
399 observed Cspk responses to an event that predicted upcoming reward. However, in the current
400 study, Cspk activity was linked to a visual cue that predicted reward delivery, whereas previously
401 we observed Cspk activity linked to an arm movement that was required to produce reward
402 delivery. Indeed, a key difference between our previous operant task and the classical
403 conditioning task studied here is that animals do not affect trial outcome with their motor output in
404 this task. Specifically, while animals learn to lick earlier after learning in this task, a change in lick
405 timing is not required for reward delivery, and there is no consequence for licks occurring with
406 'correct' or 'incorrect' timing (i.e. correctly or incorrectly matching the time of reward delivery).
407 Hence, we speculate that observed differences in Cspk activity across tasks are related to the
408 distinct sensory input and motor output that predicts reward delivery. In this task, the reward-
409 predictive event was a visual cue alone. Previously, however, despite a visual cue that instructed
410 arm movement, correct execution of the movement was required for reward delivery, and this
411 action was therefore the necessary predictor of task outcome. In support of a role for task-specific
412 movement requirements is shaping instructional signals, in the mesolimbic dopamine system it
413 has been shown with a similar operant task that dopamine release is governed by correct
414 movement initiation, and not simply reward prediction (Syed et al., 2016).
415
416 Another notable difference from our previous work is that we do not observe clear reward omission
417 responses in this task. While it is unclear why such responses are absent in the current task, we
418 again speculate that such responses may only be generated when movement is required to
419 determine task outcome. In neither task, however, did we observe decreases in Cspk activity at
420 the time when reward was expected on reward omission trials. Thus, we have not observed any
421 evidence of negative prediction errors in Cspk activity. These results contrast with a recent
422 eyeblink conditioning study that used an aversive stimulus to drive learning (Ohmae and Medina,
423 2015), and further suggests a key role for task parameters in establishing the specific features of
424 Cspk responses. Another possibility is suggested by the mesolimbic dopamine system, where
425 neurons have different response profiles depending on their striatal projection target (Menegas et
426 al., 2017; Parker et al., 2016). It thus remains possible that climbing fibers also exhibit an
427 analogous target-specific response variability, and signal diverse reward-related information such
428 as negative prediction errors in other regions of the cerebellum. Lastly, recent measurements of
429 VTA dopamine neuron responses have revealed that increased firing to reward can persist after

learning (Coddington and Dudman, 2018), similar to what we observe in Crus II. In those experiments, negative prediction errors did emerge eventually, but only very late in training, indicating that over-training can be required for omission responses to develop.

Finally, in this study we have measured Cspk responses across learning, thus revealing how Cspk activity shifts from reward-related responses to responses driven by reward predictive cues in the same animals. While we cannot rule out a contribution of sensory gating due to arousal, these data are most consistent with Cspks representing learned reward predictions. These data also suggest that the same climbing fibers can adjust their responses as a function of learning, and can signal diverse reward expectation information (i.e. both reward-predicting cues and unexpected reward in the same climbing fibers). These learned, reward-predictive climbing fiber signals are ideally suited to instruct both cerebellar learning and modulation of reward processing in downstream brain regions. In particular, a recent study has demonstrated that output from the lateral cerebellum via the deep cerebellar nuclei (DCN) forms a monosynaptic, excitatory connection onto dopamine neurons in the VTA (Carta et al., 2019). Activating these DCN projections is sufficient to positively modulate reward-driven behaviors, and these same projections are endogenously active under social conditions. These data strongly suggest that the cerebellum must contain, or have the ability to learn, information about rewarding stimuli. While speculative, such a model fits well with the observations made here. Specifically, we have shown Cspk instructional signals can become associated with stimuli that predict reward. If combined with contextual information from the mossy fiber pathway, such Cspk signals would be effective in instructing plasticity to depress Purkinje cell output and thereby enable DCN output to the VTA in response to any new, earlier reward-associated stimuli or actions. Hence, a key next step will be to evaluate the intersection of cerebellar learning with cerebellar output to the mesolimbic dopamine system during behavior. For the present, the patterns of Cspk activity demonstrated here provide key information about how instructional signals carried by cerebellar climbing fibers can change as a function of learning to signal reward expectation across the lateral cerebellum.

Methods

Mice

463 All experimental procedures using animals were carried out with the approval of the Duke
464 University Animal Care and Use Committee. All experiments were performed during light cycle
465 using adult mice (p84-205) of both sexes, randomly selected from breeding litters. All mice were
466 housed in a vivarium with normal light/dark cycles in cages with 1-5 mice. Imaging experiments
467 were performed using Tg(PCP2-Cre)3555Jdhu mice (Jackson Labs, 010536; n=34). A subset of
468 these animals (n=12) were the result of a genetic cross with Ai148(TIT2L-GC6f-ICL-tTA2)-D mice
469 (Jackson Labs, 030328). We used two exclusion criteria for animals in this study: (1) poor
470 recovery or other health concerns following surgical intervention or (2) missed virus injection, as
471 determined by *in vivo* imaging and post-hoc histological analysis.
472
473 Surgical Procedures
474 3-10 hours prior to surgery, animals received dexamethasone (3mg/kg) and ketoprofen (5mg/kg).
475 Surgical procedures were performed under anesthesia, using an initial dose of ketamine/xylazine
476 (50mg/kg and 5mg/kg) 5 minutes prior to surgery and sustained during surgery with 1.0-2.0%
477 isoflurane. Toe pinches and breathing were used to monitor anesthesia levels throughout
478 surgeries. Body temperature was maintained using a heating pad (TC-1000 CWE Inc.). Custom-
479 made titanium headplates (HE Parmer) were secured to the skull using Metabond (Parkell). For
480 imaging experiments, a 3mm diameter craniotomy was made over the lobule simplex at
481 approximately 1.4mm lateral and 2.8mm posterior to lambda or crus I and II at approximately
482 3.0mm lateral and 4.3mm posterior to lambda. Glass cover slips consisting of two 3mm bonded
483 to a 5mm coverslip (Warner Instruments No. 1) with index matched adhesive (Norland No. 1)
484 were secured in the craniotomy using Metabond. Buprenex (0.05mg/kg) and cefazolin (50mg/kg)
485 were administered following surgery twice a day for two days. Following a minimum of 4 recovery
486 days, animals were water deprived for 3 days, or until body weight stabilized at 85% of initial
487 weight, and were habituated to head restraint (3-5 days) prior to behavioral training.
488
489 For imaging experiments involving viral expression of GCaMP (all non-Ai148 animals), the glass
490 cover slip was removed following behavioral training, and mice were injected (WPI UMP3) with
491 AAV1.CAG.Flex.GCaMP6f.WPRE.SV40 (UPenn vector core, titer = 1.48×10^{13} or 7.60×10^{12}). 150
492 nL virus diluted 1:1-1:5 in ACSF was injected at a rate of 30nl/min and a depth of 150 μm at 1-3
493 sites in dorsal lobule simplex. A new cranial window was then implanted, and imaging was
494 performed beginning 10-14 days following injection. Transgenic mice crossed with the Ai148
495 mouse line received no injection and were given 10 days to recover from surgery before training.
496

497 Behavior

498 During behavioral training, animals were head-fixed and placed in front of a computer monitor
499 and reward delivery tube. Animals were trained to associate a visual cue with a saccharine
500 reward. A high contrast vertical black and white grating was present at all times, including the
501 inter-trial interval (ITI; 24-30 s), except when the reward cue was presented. The reward cue
502 consisted of a horizontal grating, presented for 100ms, and followed reward delivery after a 500ms
503 delay (600 ms from cue onset)(Heffley et al., 2018). Training sessions lasted for 62.1 ±0.9 minutes
504 and consisted of 130.1 ±1.8 trials (n = 134 sessions). Imaging sessions lasted an average of 63.0
505 ±1.2 minutes and consisted of 128.5 ±2.5 trials (n = 71 sessions). For reward omission sessions,
506 20% of randomly determined trials were unrewarded. For unexpected reward sessions, no reward
507 cue was presented on 20% of randomly determined trials. Behavioral parameters including cue
508 presentation, reward delivery, and licking were monitored using Mworks (http://mworks-
509 project.org) and custom software written in MATLAB (Mathworks). Learning was defined by
510 stabilization of reaction times and miss rates, with required reaction times less than 650 ms and
511 a miss rate below 15%. Across animals, 5.7 ± 0.4 training sessions (n = 27 mice imaged on both
512 Day 1 and Day N+1) was required to meet these criteria. In a subset of experiments, (5 mice in
513 LS, 3 mice in Crus I & II), we used a piezoelectric sensor (C.B. Gitty, 41 mm "jumbo" piezo)
514 integrated into the behavioral apparatus to measure animal movement.

515

516 Calcium Imaging

517 *Mesoscale imaging*: Single photon imaging was performed using a customized microscope
518 (Sutter SOM) affixed with a 5x objective (Mitutoyo, 0.14NA) and CMOS camera (Qimaging, Rolera
519 em-c^2). Excitation (470 nm) was provided by an LED (ThorLabs, M470L3), and data were
520 collected through a green filter (520-536 nm band pass, Edmund Optics) at a frame rate of 10Hz,
521 with a field of view of 3.5x3.5mm at 1002x1004 pixels.

522

523 *Two-Photon Imaging*: Two-photon imaging was performed with a resonant scanning microscope
524 (Neurolabware) using a 16x water immersion objective (Nikon CFI75 LWD 16xW 0.80NA).
525 Imaging was performed using a polymer to stabilize the immersion solution (MakingCosmetics,
526 0.4% Carbomer 940). A Ti:Sapphire laser tuned to 920nm (Spectra Physics, Mai Tai eHP
527 DeepSee) was raster scanned via a resonant galvanometer (8 kHz, Cambridge Technology) at a
528 frame rate of 30 Hz with a field of view of 1030 μm x 581 μm (796 x 264 pixels). Data were
529 collected through a green filter (510 ± 42 nm band filter (Semrock) onto GaAsP photomultipliers
530 (H10770B-40, Hamamatsu) using Scanbox software (Neurolabware). Experiments were aborted

531 if significant z-motion was evident during recording. A total of 29 mice were used for imaging
532 experiments across lobules in Figures 2-6 (6 mice for mesoscale imaging in LS; 16 mice for two-
533 photon imaging in LS; 7 mice for two-photon imaging in Crus I and Crus II (both lobules imaged
534 in the same mice). In these experiments, the range of contributing dendrites to each experiment
535 was as follows: LS: Day 1, 26-106 dendrites, 15 mice; Day N+1, 20-103 dendrites, 16 mice; Day
536 N+2, 15-82 dendrites, 6 mice; Crus I: Day 1, 6-57 dendrites, 6 mice; Day N+1, 10-43 dendrites, 7
537 mice; Day N+2, 10-57 dendrites, 5 mice; Crus II: Day 1, 18-40 dendrites, 5 mice; Day N+1, 24-78
538 dendrites, 6 mice; Day N+2, 10-46 dendrites, 6 mice. 5 additional mice (separate cohort) were
539 used to collect piezoelectric movement data on day N+1 for LS during imaging. For these
540 experiments, the range of dendrites across experiments was 32-101. Piezoelectric movement
541 data for Crus I and II came from a subset of the main cohort of animals described above.
542
543 Data Analysis and Statistics
544 *Behavior:* Analysis was performed using custom MATLAB code. Reaction times were defined as
545 the first lick occurring 200-1000ms after reward cue onset. Miss rate was defined as the percent
546 of trials without a lick in the 1s following cue presentation.
547
548 *Mesoscale imaging:* Imaging analysis was performed using custom MATLAB code. Regions of
549 interest (ROIs) were selected within LS according to the pattern of GCaMP expression. Window
550 location and the lobule identity were identified according to folia patterns visible through the
551 cranial window, landmarks recorded during surgery, and post-hoc histology. Baseline
552 fluorescence (F) was measured on a trial-by-trial basis during the ITI as the mean F between 900
553 and 200ms before trial initiation. Normalized fluorescence ($\Delta F/F$) was calculated according to the
554 cumulative activity within an ROI. $\Delta F/F$ latency was measured by first finding the peak $\Delta F/F$
555 response following cue onset averaged across trials. Next, the latency was measured as the time
556 when mean $\Delta F/F$ trace achieved a maximum rate of change (the peak of the first derivative) in a
557 500ms window preceding the identified peak $\Delta F/F$ response.
558
559 *Two-photon imaging*: Motion in the X and Y planes was corrected by sub-pixel image registration.
560 No data was excluded (after collection, see above) due to z-axis motion (assessed in each
561 experiment by reviewing the trial averaged, cue aligned movie after X-Y motion correction). To
562 isolate signals from individual PC dendrites, we utilized principal component analysis (PCA)
563 followed by independent component analysis (ICA). Final dendrite segmentation was achieved
564 by thresholding the smoothed spatial filters from ICA. A binary mask was created by combining

565 highly correlated pixels (correlation coefficient > 0.8) and removing any overlapped regions
566 between segmented dendrites. Notably, image segmentation using these criteria did not extract
567 PC soma, which were clearly visible in some two-photon imaging experiments. Fluorescence
568 changes (ΔF) were normalized to a window of baseline fluorescence (F) between 500ms and
569 100ms preceding trial initiation. One experiment was excluded from analysis based on single trial
570 $\Delta F/F$ values that were more than double the amplitude of any other experiment, according to the
571 rationale that any increases in Cspk activity during learning could be obscured by indicator
572 saturation.
573
574 To extract events corresponding to Cspks, the first derivative of the raw fluorescence trace was
575 thresholded at 1.7 standard deviations from baseline. Events above this threshold were variable
576 in amplitude (Fig. 3- Supplement 1, also described previously, (Heffley et al., 2018)). Previous
577 work has demonstrated that calcium transient amplitude variability reflects the properties of
578 climbing fiber input, and not a combined climbing fiber and parallel fiber signal (Gaffield et al.,
579 2019; Gaffield et al., 2018). All events separated by at least one frame were included. The pre-
580 reward window was defined as the 600 ms between the cue and the reward delivery; the post-
581 reward window was defined as the 600 ms following reward (or the time of expected reward).
582 Peak spike rates for individual PC dendrites were defined by first identifying the peak spike rate
583 in the mean peri-stimulus histogram (PSTH) across all PC dendrites within either the Pre- or Post-
584 reward window. Next, this peak was used to define a 100 ms analysis window centered on the
585 peak, to calculate spike rate. To identify PC dendrites responsive at the time of this peak, we
586 selected only those PC dendrites with a peak response at least one standard deviation above
587 their pre-cue baseline activity. To determine whether responses were significant across the
588 population, we compared the responses of all PC dendrites at the time of the peak in the PSTH
589 to a peak found in a 1200 ms window during the baseline and performed a one-tailed t-test across
590 PC dendrites.
591
592 To identify PC dendrites that were responsive to task events (i.e. visual cue or reward), we
593 selected PC dendrites with spike rates that were elevated 1 standard deviation above the pre-cue
594 period for two consecutive frames in the pre- or post-reward windows. To identify PC dendrites
595 that were suppressed following expected reward, we selected PC dendrites with spike rates that
596 were suppressed 1 standard deviation below both their pre-cue and pre-reward firing rates for
597 two consecutive frames during the post-reward window. These criteria selected a very small

number of dendrites, which upon inspection, revealed no clear suppression associated with the time of expected reward (**Fig. 3 – Figure Supplement 3**).

Single licks during the ITI (separated by at least 250 ms from other licks) were used to generate lick triggered averages; only experiments with at least 4 licks were included for this analysis. Peaks in the lick triggered average were identified within a window spanning 5 frames centered on the lick. Significance was calculated by comparing the amplitude of this peak with two frames 250 ms before the lick and two frames 250 ms after the lick. To segregate trials according to lick times, on each trial we identified the first lick bout (at least 3 licks within 300 ms) following the cue, and separated trials into quartiles according to lick latency.

To track single PC dendrites across imaging sessions, we first independently generated pixel masks for PC dendrites from each field of view. We then motion registered the mean fluorescence image from the post-learning session to the pre-learning session, and applied the same pixel shifts from this registration to the segmented pixel masks from the post-learning condition. By overlaying the shifted post-learning pixel masks with the pre-learning masks, we assessed the overlap between imaging days. We employed a stringent criterion of greater than 50% overlap to increase the probability of accurately identifying the same PC dendrites across imaging sessions. With these criteria, we identified a group of PC dendrites likely corresponding to the same neurons before and after learning.

Additional statistics: Data are presented as mean ± S.E.M., unless stated otherwise. Statistical tests were two-sided, except as specifically noted. Differences were considered statistically significant when $P < 0.05$. No correction for multiple comparisons was applied. No statistical methods were used to predetermine sample sizes. Data distribution was assumed to be normal but this was not formally tested. Data collection and analysis were not performed blind to the conditions of the experiments, but data collection relied on automatized measurements and subsequent analysis was based on code uniformly applied across experimental conditions.

Acknowledgements

This work was supported by grants from the NIH NINDS (5R01NS096289-02) (CH) and (F31NS103425) (WH), the Sloan Foundation (CH), and the Whitehall Foundation (CH). We thank L. Glickfeld for helpful discussions and input on calcium imaging approaches and analyses, and members of the Hull and Glickfeld labs for input and technical assistance throughout the project.

632

633 **Author Contributions**

634 WH and CH designed experiments, WH conducted experiments, WH and CH analyzed data, and
635 WH and CH wrote the manuscript.

636

637 **Competing Interests**

638 The authors declare no competing interests.

639

640

641 **Figure Legends**

642

643 **Figure 1**. Appetitive classical conditioning regime for head-fixed mice. **(A)** Diagram of headplate
644 and 3mm cranial window. **(B)** Scale representation of the 3mm cranial windows over either Lobule
645 Simplex (LS) or Crus I and II. **(C)** Mice viewed a static full screen vertical grating that was
646 transiently replaced by a horizontal grating for 100ms to cue reward delivery following a 600ms
647 delay. **(D)** Trial structure and progression of learning sessions. **(E)** Left, mean reaction time,
648 defined as the first lick following the visual cue, on rewarded trials across training days. Right,
649 mean reaction time on rewarded trials before learning and after learning. **(F)** Left, mean miss
650 rate, defined as the fraction of trials with no licks within 1 s after the cue, on rewarded trials across
651 training days. Right, mean miss rate on rewarded trials before and after learning **(G)** Mean lick
652 rates aligned to visual cue onset, before (top) and after (bottom) learning for rewarded trials (RW,
653 left) and omission trials (right, dotted line indicates time when reward would have been delivered).

654

655 **Figure 2**. Single photon, mesoscale imaging of Cspk activity during behavior. **(A)** Schematic of
656 the cerebellar cortex with GCaMP6f expressed in PCs for single or two photon dendrite imaging.
657 **(B)** Average $\Delta F/F$ timecourse (black, collected at 10Hz) and lick rate (blue bars) for an example
658 animal before (top) and after (bottom) learning for rewarded (left) and reward omission (right)
659 trials. **(C,D,E)** Summary of bulk Cspk response latencies relative to the visual cue **C,D** or the
660 reward **E** for all trial types. Response latency is defined by the maximum positive change in $\Delta F/F$
661 rate within 500ms before the peak response.

662

663 **Figure 3**. Cspk modulation in LS across learning. **(A)** $\Delta F/F$ timecourses from an example neuron
664 measured via two-photon calcium imaging for the first day of training in naive mice. Grey traces
665 are the first 50 trials and the black trace is the average of those 50 trials. **(B)** Same as **A**, but on

post-learning day N+1. **(C)** Same as **A,B** but for post-learning day N+2. **(D)** Top, mean cue-aligned peri-stimulus histograms (PSTHs) of Cspk rate on reward (black) and omission (red) trials for all PC dendrites on the first day of training in naïve mice. Bottom, summary scatterplot comparing the Cspk rate for individual PCs on rewarded vs omission trials in naïve mice. Spike rates were measured in a window preceding reward delivery (left) or immediately after reward delivery (right) (methods). **(E)** Same as **D**, but for rewarded and reward omission trials on post-learning day N +1 **(F)** Same as **D,E**, but for rewarded and unexpected reward trials on post-learning day N+2. **(G)** Mean cue-aligned PSTH for PC dendrites that exhibited Cspk responses to the visual cue. *Inset*: fraction of the total dendrites on Day N+2 that responded in the pre-reward window on rewarded trials only (light blue, 24%), the post-reward window on unexpected reward trials only (yellow, 7%), both pre and post reward windows on rewarded and unexpected reward trials respectively (green, 10%), and neither window (blue, 58%). **(H)** Mean lick-triggered PSTH for licks during the inter-trial interval (ITI) in naïve animals. **(I)** Mean cue-aligned PSTHs for trained animals with rewarded trials segregated according to trials with the earlies 1/4 of licks (black, 162 ± 19 ms from cue) and latest 1/4 of licks (blue, 604 ± 64 ms from cue). **(J)** Mean cue-aligned PSTHs for trained animals with rewarded trials segregated according to trials with the highest 1/4 of lick rates (black, 5.4 ± 0.1 Hz) and the lowest 1/4 of lick rates (blue, 2.6 ± 0.1 Hz). **(K)** Fraction of all lobule simplex neurons which were responsive to specific task events on the first day of training for rewarded trials (left) and all trials (right). **(L)** Same as **K** but for training day N+1. Data points with horizontal error bars represent the mean lick timing ± SEM. For all PSTHs, shaded area represents ± SEM across dendrites.

Figure 4. Cspk responses measured in the same fields of view across learning. **(A)** Example of manual identification from a field of view containing several of the same PC dendrites on day 1 and day N+1. Left, fields of view for day 1 (top) and day N+1 (bottom). Right, magnified view from the white box at left. Red arrows indicate an example PC dendrite identified both pre and post learning. Scale bars are 200 μm (x) x 50 μm (y). **(B)** Cue aligned calcium transients averaged across trials extracted from the PC dendrite identified in **A** for day 1 (top) and day N+1 (bottom). **(C)** Mean images taken from day 1 (left) and day N+1 (right) after independent rigid motion registration on each dataset. Scale bars are 200 μm (x) x 50 μm (y). **(D)** Pixel masks of PC dendrites independently extracted from the datasets in **C** (methods). **(E)** The post-learning data set from **C**, right, was motion registered to the pre-learning dataset from **C**, left. The resulting x-y pixel shifts were applied to the post-learning dendrite pixel masks from **D**, right. **(F,G)** Following registration, the overlap between pre and post learning pixel masks was compared quantitatively

700 **F** and graphically **G**, with pre-learning masks labeled red, post-learning masks labeled green, and
701 overlap labeled yellow. **(H)** Dendritic masks from **G** which had >50% overlap. **(I)** Summary of Cspk
702 firing rates for individual PC dendrites in the pre (left) and post (right) reward window for all
703 dendrites which had a >50% overlap in their dendritic masks across learning (n=61). **(J)** Summary
704 of Cspk rates for the same individual PC dendrites in **I,** measured in the post-reward window on
705 Day 1 and the pre-reward window on Day N+1.
706
707 **Figure 5**. Cspk modulation in Crus I across learning. **(A)** ∆F/F timecourses from an example
708 neuron measured via two-photon calcium imaging for the first day of training in naive mice. Grey
709 traces are the first 50 trials and the black trace is the average of those 50 trials. **(B)** Same as **A**,
710 but on post-learning day N+1. **(C)** Same as **A,B** but for post-learning day N+2. **(D)** Top, mean
711 cue-aligned PSTHs of Cspk rate on reward (black) and omission (red) trials for all PC dendrites
712 on the first day of training in naïve mice. Bottom, summary scatterplot comparing the Cspk rate
713 for individual PCs on rewarded vs omission trials in naïve mice. Spike rates were measured in a
714 window preceding reward delivery (left) or immediately after reward delivery (right) (methods). **(E)**
715 Same as **D**, but for rewarded and reward omission trials on post-learning day N +1 **(F)** Same as
716 **D,E**, but for rewarded and unexpected reward trials on post-learning day N+2. **(G)** Mean cue-
717 aligned PSTH for PC dendrites that exhibited Cspk responses to the visual cue. *Inset*: fraction of
718 the total dendrites on Day N+2 that responded in the pre-reward window on rewarded trials only
719 (light blue, 51%), the post-reward window on unexpected reward trials only (yellow, 3%), both pre
720 and post reward windows on rewarded and unexpected reward trials respectively (green, 20%),
721 and neither window (blue, 26%). **(H)** Mean lick-triggered PSTH for licks during the ITI in naïve
722 animals. **(I)** Mean cue-aligned PSTHs for trained animals with rewarded trials segregated
723 according trials with the earlies 1/4 of licks (black, 326 ± 46 ms from cue) and latest 1/4 of licks
724 (blue, 1010 ± 34 ms from cue). **(J)** Mean cue-aligned PSTHs for trained animals with rewarded
725 trials segregated according to trials with the highest 1/4 of lick rates (black, 4.8 ± 0.1 Hz) and the
726 lowest 1/4 of lick rates (blue, 2.1 ± 0.1 Hz) following reward delivery. **(K)** Fraction of all Crus I
727 neurons which were responsive to specific task events on the first day of training for rewarded
728 trials (left) and all trials (right). **(L)** Same as **K** but for training day N+1. Data points with horizontal
729 error bars represent the mean lick timing ± SEM. For all PSTHs, shaded area represents ± SEM
730 across dendrites.
731
732 **Figure 6**. Cspk modulation in Crus II across learning. **(A)** ∆F/F timecourses from an example
733 neuron measured via two-photon calcium imaging for the first day of training in naive mice. Grey

traces are the first 50 trials and the black trace is the average of those 50 trials. **(B)** Same as **A**, but on post-learning day N+1. **(C)** Same as **A,B** but for post-learning day N+2. **(D)** Top, mean cue-aligned PSTHs of Cspk rate on reward (black) and omission (red) trials for all PC dendrites on the first day of training in naïve mice. Bottom, summary scatterplot comparing the Cspk rate for individual PCs on rewarded vs omission trials in naïve mice. Spike rates were measured in a window preceding reward delivery (left) or immediately after reward delivery (right) (methods). **(E)** Same as **D**, but for rewarded and reward omission trials on post-learning day N +1 **(F)** Same as **D,E**, but for rewarded and unexpected reward trials on post-learning day N+2. **(G)** Mean cue-aligned PSTH for PC dendrites that exhibited Cspk responses to the visual cue on Day N+2. *Inset*: fraction of the total dendrites on Day N+2 that responded in the pre-reward window on rewarded trials only (light blue, 19%), the post-reward window on unexpected reward trials only (yellow, 10%), both pre and post reward windows on rewarded and unexpected reward trials respectively (green, 14%), and neither window (blue, 57%). **(H)** Mean lick-triggered PSTH for licks during the ITI in naïve animals. **(I)** Mean cue-aligned PSTHs for trained animals with rewarded trials segregated according trials with the earlies 1/4 of licks (black, 296 ± 52 ms from cue) and latest 1/4 of licks (blue, 914 ± 78 ms from cue). **(J)** Mean cue-aligned PSTHs for trained animals with rewarded trials segregated according to trials with the highest 1/4 of lick rates (black, 5.0 ± 0.2 Hz) and the lowest 1/4 of lick rates (blue, 2.5 ± 0.2 Hz) following reward delivery. **(K)** Fraction of all Crus II neurons which were responsive to specific task events on the first day of training for rewarded trials (left) and all trials (right). **(L)** Same as **K** but for training day N+1. Data points with horizontal error bars represent the mean lick timing ± SEM. For all PSTHs, shaded area represents ± SEM across dendrites.

Figure 7. Body movements do not explain the learned reward predictive Cspks **(A)** Piezoelectric movement sensor was used to measure movements during the behavior for a subset of animals. **(B)** movement traces corresponding to mouse breathing during awake (top) and anaesthetized (bottom) conditions. Note that breathing becomes both slower and deeper (larger amplitude movements) under anesthesia. **(C)** Top, movement traces for the 10% of trials with the most (black) and least (blue) movement in the pre-reward window. Bottom, mean cue-aligned PSTHs from PCs in the lobule simplex corresponding to the subset of trials with the most (black) and least (blue) movement. **(D)** Same as **B** but for Crus I. **(E)** Same as **B,C** but for Crus II. For all PSTHs, shaded area represents ± SEM across dendrites.

767 **Fig. 3– Figure Supplement 1** Comparison of the mean ΔF/F response for all neurons segregated
768 according to lobule, pre vs post learning, and pre vs post reward delivery.
769
770 **Fig. 3 – Figure Supplement 2.** A minority of PC dendrites can respond to reward and the reward-
771 predictive cue after learning. **(A)** Mean cue-aligned PSTH for PC dendrites that exhibited Cspk
772 responses to reward. **(B)** Mean cue-aligned PSTH for PC dendrites that did not exhibit Cspk
773 responses to reward.
774
775 **Fig. 3 – Figure Supplement 3.** No evidence of Cspk suppression following reward omission.
776 **(A-C)** Cspk responses identified as suppressed below baseline according to statistical criteria
777 (methods) in LS, Crus I and Crus II show no suppression upon visual inspection. These small
778 numbers of PC dendrites were likely identified based on noise in the PSTHs that crossed the
779 threshold for significance.
780
781 **References**
782
783 Ackermann, H. (2008). Cerebellar contributions to speech production and speech perception:
784 psycholinguistic and neurobiological perspectives. Trends Neurosci 31, 265-272.
785 Albus, J.S. (1971). A theory of cerebellar function. Mathematical Biosciences 10, 25-61.
786 Apps, R., and Garwicz, M. (2005). Anatomical and physiological foundations of cerebellar
787 information processing. Nat Rev Neurosci 6, 297-311.
788 Apps, R., and Hawkes, R. (2009). Cerebellar cortical organization: a one-map hypothesis. Nat
789 Rev Neurosci 10, 670-681.
790 Badura, A., Verpeut, J.L., Metzger, J.W., Pereira, T.D., Pisano, T.J., Deverett, B., Bakshinskaya,
791 D.E., and Wang, S.S. (2018). Normal cognitive and social development require posterior
792 cerebellar activity. Elife 7.
793 Brown, S.T., and Raman, I.M. (2018). Sensorimotor Integration and Amplification of Reflexive
794 Whisking by Well-Timed Spiking in the Cerebellar Corticonuclear Circuit. Neuron 99, 564-575
795 e562.
796 Bryant, J.L., Boughter, J.D., Gong, S., LeDoux, M.S., and Heck, D.H. (2010). Cerebellar cortical
797 output encodes temporal aspects of rhythmic licking movements and is necessary for normal
798 licking frequency. Eur J Neurosci 32, 41-52.
799 Carta, I., Chen, C.H., Schott, A.L., Dorizan, S., and Khodakhah, K. (2019). Cerebellar modulation
800 of the reward circuitry and social behavior. Science (New York, NY) 363, eaav0581.

801 Chen, S., Augustine, G.J., and Chadderton, P. (2016). The cerebellum linearly encodes whisker
802 position during voluntary movement. Elife 5, e10509.
803 Chen, S., Augustine, G.J., and Chadderton, P. (2017). Serial processing of kinematic signals by
804 cerebellar circuitry during voluntary whisking. Nat Commun 8, 232.
805 Coddington, L.T., and Dudman, J.T. (2018). The timing of action determines reward prediction
806 signals in identified midbrain dopamine neurons. Nature Neuroscience 21, 1563-1573.
807 Deverett, B., Koay, S.A., Oostland, M., and Wang, S.S. (2018). Cerebellar involvement in an
808 evidence-accumulation decision-making task. Elife 7.
809 Gaffield, M.A., Amat, S.B., Bito, H., and Christie, J.M. (2016). Chronic imaging of movement-
810 related Purkinje cell calcium activity in awake behaving mice. J Neurophysiol 115, 413-422.
811 Gaffield, M.A., Bonnan, A., and Christie, J.M. (2019). Conversion of Graded Presynaptic Climbing
812 Fiber Activity into Graded Postsynaptic Ca(2+) Signals by Purkinje Cell Dendrites. Neuron 102,
813 762-769 e764.
814 Gaffield, M.A., and Christie, J.M. (2017). Movement Rate Is Encoded and Influenced by
815 Widespread, Coherent Activity of Cerebellar Molecular Layer Interneurons. J Neurosci 37, 4751-
816 4765.
817 Gaffield, M.A., Rowan, M.J.M., Amat, S.B., Hirai, H., and Christie, J.M. (2018). Inhibition gates
818 supralinear Ca(2+) signaling in Purkinje cell dendrites during practiced movements. Elife 7.
819 Heffley, W., Song, E.Y., Xu, Z., Taylor, B.N., Hughes, M.A., McKinney, A., Joshua, M., and Hull,
820 C. (2018). Coordinated cerebellar climbing fiber activity signals learned sensorimotor predictions.
821 Nature Neuroscience 21, 1431-1441.
822 Hoshi, E., Tremblay, L., Féger, J., Carras, P.L., and Strick, P.L. (2005). The cerebellum
823 communicates with the basal ganglia. Nature neuroscience 8, 1491-1493.
824 Ito, M. (1972). Neural design of the cerebellar motor control system. Brain Res 40, 81-84.
825 Ivry, R.B., and Spencer, R.M. (2004). The neural representation of time. Curr Opin Neurobiol 14,
826 225-232.
827 Ju, C., Bosman, L.W.J., Hoogland, T.M., Velauthapillai, A., Murugesan, P., Warnaar, P., van
828 Genderen, R.M., Negrello, M., and De Zeeuw, C.I. (2019). Neurons of the inferior olive respond
829 to broad classes of sensory input while subject to homeostatic control. J Physiol 597, 2483-2514.
830 Kim, S.G., Ugurbil, K., and Strick, P.L. (1994). Activation of a cerebellar output nucleus during
831 cognitive processing. Science 265, 949-951.
832 Kitazawa, S., Kimura, T., and Yin, P.-B. (1998). Cerebellar complex spikes encode both
833 destinations and errors in arm movements. Nature 392, 494-497.

834 Kostadinov, D., Beau, M., Pozo, M.B., and Hausser, M. (2019). Predictive and reactive reward
835 signals conveyed by climbing fiber inputs to cerebellar Purkinje cells. Nat Neurosci 22, 950-962.
836 Larry, N., Yarkoni, M., Lixenberg, A., and Joshua, M. (2019). Cerebellar climbing fibers encode
837 expected reward size. bioRxiv, 533653.
838 Marr, D. (1969). A theory of cerebellar cortex. The Journal of Physiology 202, 437-470.
839 McAfee, S.S., Liu, Y., Sillitoe, R.V., and Heck, D.H. (2019). Cerebellar Lobulus Simplex and Crus
840 I Differentially Represent Phase and Phase Difference of Prefrontal Cortical and Hippocampal
841 Oscillations. Cell Rep 27, 2328-2334 e2323.
842 Menegas, W., Babayan, B.M., Uchida, N., and Watabe-Uchida, M. (2017). Opposite initialization
843 to novel cues in dopamine signaling in ventral and posterior striatum in mice. Elife 6.
844 Mothersill, O., Knee-Zaska, C., and Donohoe, G. (2016). Emotion and Theory of Mind in
845 Schizophrenia-Investigating the Role of the Cerebellum. Cerebellum 15, 357-368.
846 Ohmae, S., and Medina, J.F. (2015). Climbing fibers encode a temporal-difference prediction
847 error during cerebellar learning in mice. Nature Neuroscience 18, 1798-1803.
848 Parker, N.F., Cameron, C.M., Taliaferro, J.P., Lee, J., Choi, J.Y., Davidson, T.J., Daw, N.D., and
849 Witten, I.B. (2016). Reward and choice encoding in terminals of midbrain dopamine neurons
850 depends on striatal target. Nat Neurosci 19, 845-854.
851 Proville, R.D., Spolidoro, M., Guyon, N., Dugue, G.P., Selimi, F., Isope, P., Popa, D., and Lena,
852 C. (2014). Cerebellum involvement in cortical sensorimotor circuits for the control of voluntary
853 movements. Nat Neurosci 17, 1233-1239.
854 Reis, D.J., Doba, N., and Nathan, M.A. (1973). Predatory attack, grooming, and consummatory
855 behaviors evoked by electrical stimulation of cat cerebellar nuclei. Science 182, 845-847.
856 Schmahmann, J.D. (1991). An emerging concept. The cerebellar contribution to higher function.
857 Arch Neurol 48, 1178-1187.
858 Schmahmann, J.D., and Caplan, D. (2006). Cognition, emotion and the cerebellum. Brain 129,
859 290-292.
860 Schmahmann, J.D., Guell, X., Stoodley, C.J., and Halko, M.A. (2019). The Theory and
861 Neuroscience of Cerebellar Cognition. Annu Rev Neurosci.
862 Schultz, W., Dayan, P., and Montague, P.R. (1997). A neural substrate of prediction and reward.
863 Science (New York, NY) 275, 1593-1599.
864 Streng, M.L., Popa, L.S., and Ebner, T.J. (2017). Climbing fibers predict movement kinematics
865 and performance errors. J Neurophysiol 118, 1888-1902.

866 Syed, E.C.J., Grima, L.L., Magill, P.J., Bogacz, R., Brown, P., and Walton, M.E. (2016). Action
867 initiation shapes mesolimbic dopamine encoding of future rewards. Nature Neuroscience 19, 34-
868 36.
869 Van Overwalle, F., Baetens, K., Marien, P., and Vandekerckhove, M. (2014). Social cognition and
870 the cerebellum: a meta-analysis of over 350 fMRI studies. Neuroimage 86, 554-572.
871 Wagner, M.J., Kim, T.H., Savall, J., Schnitzer, M.J., and Luo, L. (2017). Cerebellar granule cells
872 encode the expectation of reward. Nature 544, 96-100.
873 Wang, S.S., Kloth, A.D., and Badura, A. (2014). The cerebellum, sensitive periods, and autism.
874 Neuron 83, 518-532.
875 Welsh, J.P., Lang, E.J., Suglhara, I., and Llinas, R. (1995). Dynamic organization of motor control
876 within the olivocerebellar system. Nature 374, 453-457.

877

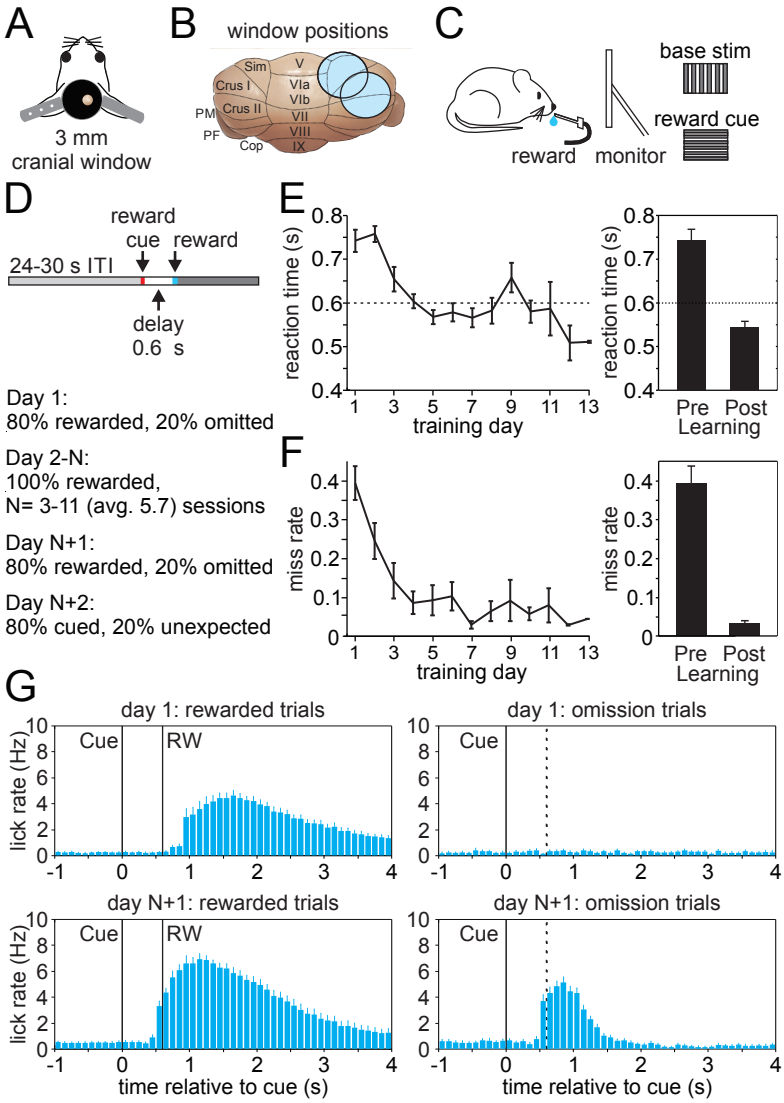
A
3 mm
cranial window
B
window positions
Sim
V
Crus I
VIa
VIb
Crus II
PM
VII
PF
VIII
Cop
IX
C
base stim
reward cue
reward
monitor
D
reward
cue
reward
24-30 s ITI
delay
0.6 s
Day 1:
80% rewarded, 20% omitted
Day 2-N:
100% rewarded,
N= 3-11 (avg. 5.7) sessions
Day N+1:
80% rewarded, 20% omitted
Day N+2:
80% cued, 20% unexpected
E
reaction time (s)
training day
Pre
Post
Learning
F
miss rate
training day
Pre
Post
Learning
G
day 1: rewarded trials
day 1: omission trials
day N+1: rewarded trials
day N+1: omission trials
Cue
RW
lick rate (Hz)
time relative to cue (s)

Figure 1

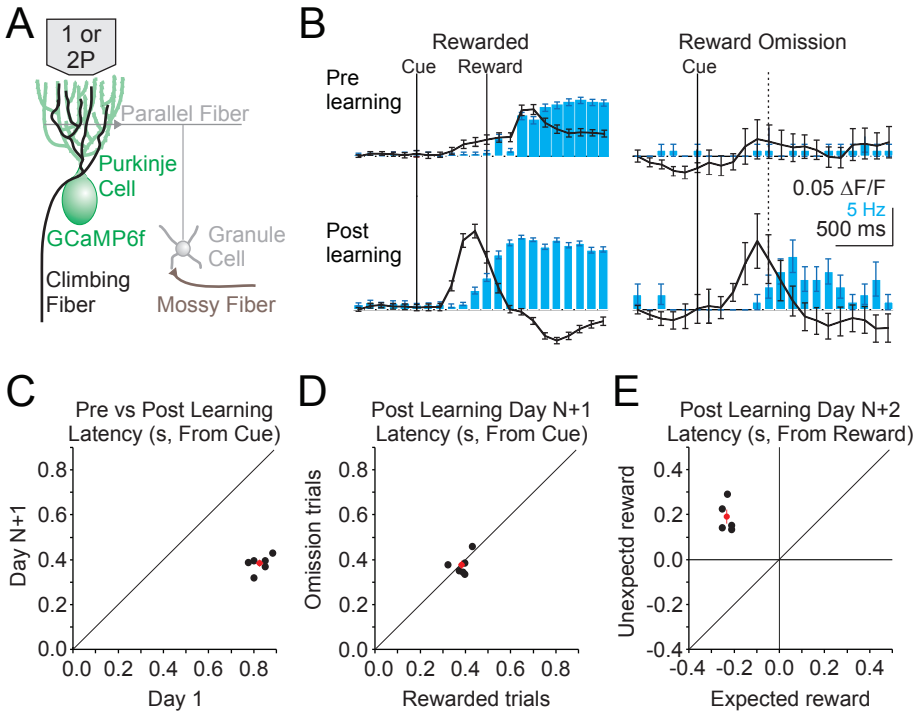
A
1 or 2P
Parallel Fiber
Purkinje Cell
GCaMP6f
Granule Cell
Climbing Fiber
Mossy Fiber
B
Rewarded
Cue
Reward
Reward Omission
Cue
Pre learning
Post learning
0.05 ΔF/F
5 Hz
500 ms
C
Pre vs Post Learning
Latency (s, From Cue)
Day N+1
Day 1
D
Post Learning Day N+1
Latency (s, From Cue)
Omission trials
Rewarded trials
E
Post Learning Day N+2
Latency (s, From Reward)
Unexpectd reward
Expected reward

Figure 2

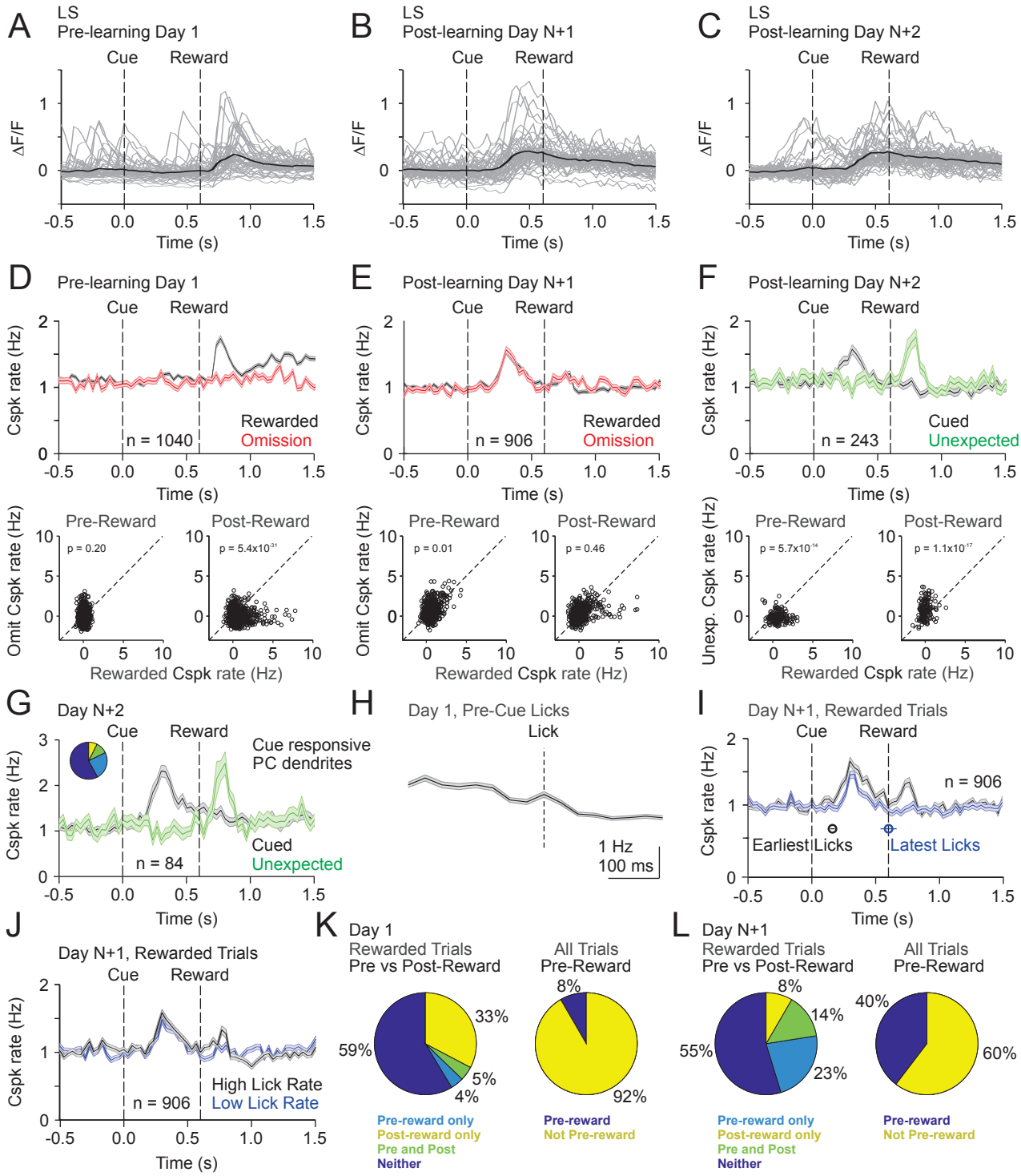
A
LS
Pre-learning Day 1
Cue
Reward
ΔF/F
Time (s)
B
LS
Post-learning Day N+1
C
LS
Post-learning Day N+2
D
Pre-learning Day 1
Cspk rate (Hz)
n = 1040
Rewarded
Omission
E
Post-learning Day N+1
n = 906
F
Post-learning Day N+2
n = 243
Cued
Unexpected
Pre-Reward
Post-Reward
p = 0.20
p = 5.4x10-31
p = 0.01
p = 0.46
p = 5.7x10-14
p = 1.1x10-17
Omit Cspk rate (Hz)
Unexp. Cspk rate (Hz)
Rewarded Cspk rate (Hz)
G
Day N+2
Cue responsive
PC dendrites
n = 84
H
Day 1, Pre-Cue Licks
Lick
1 Hz
100 ms
I
Day N+1, Rewarded Trials
Earliest Licks
Latest Licks
J
Day N+1, Rewarded Trials
High Lick Rate
Low Lick Rate
K
Day 1
Rewarded Trials
Pre vs Post-Reward
All Trials
Pre-Reward
33%
59%
5%
4%
8%
92%
Pre-reward only
Post-reward only
Pre and Post
Neither
Pre-reward
Not Pre-reward
L
Day N+1
Rewarded Trials
Pre vs Post-Reward
All Trials
Pre-Reward
8%
14%
55%
23%
40%
60%

Figure 3

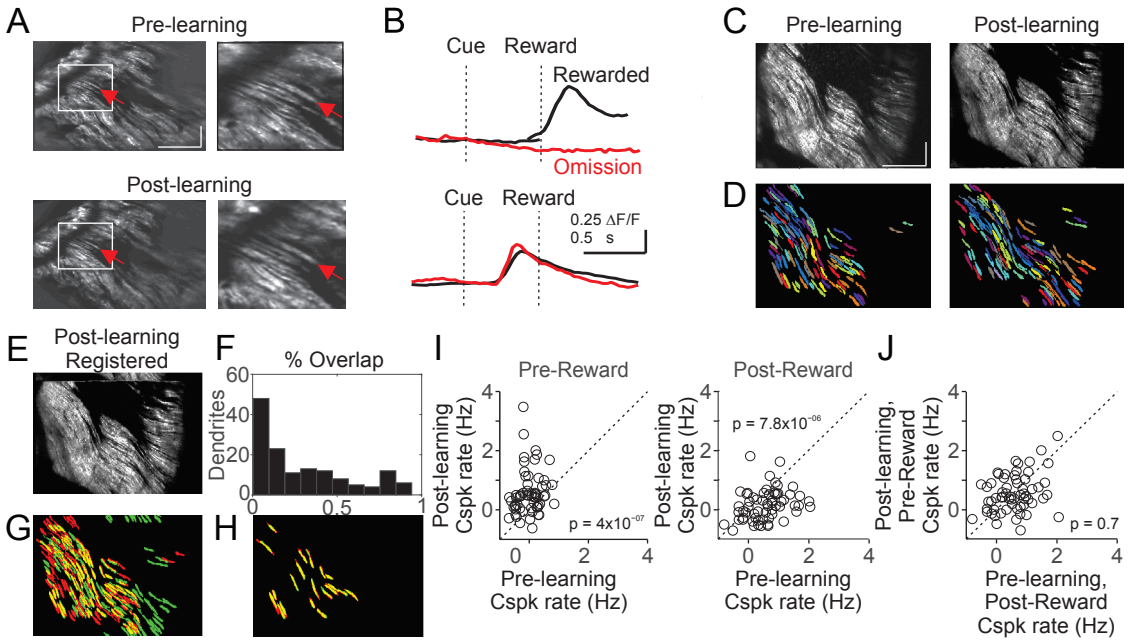
A
Pre-learning
Post-learning
B
Cue
Reward
Rewarded
Omission
Cue
Reward
0.25 ΔF/F
0.5 s
C
Pre-learning
Post-learning
D
E
Post-learning
Registered
F
% Overlap
Dendrites
60
40
20
0
0
0.5
1
G
H
I
Pre-Reward
Post-Reward
Post-learning
Cspk rate (Hz)
Pre-learning
Cspk rate (Hz)
p = 4x10^-07
p = 7.8x10^-06
J
Post-learning,
Pre-Reward
Cspk rate (Hz)
Pre-learning,
Post-Reward
Cspk rate (Hz)
p = 0.7

Figure 4

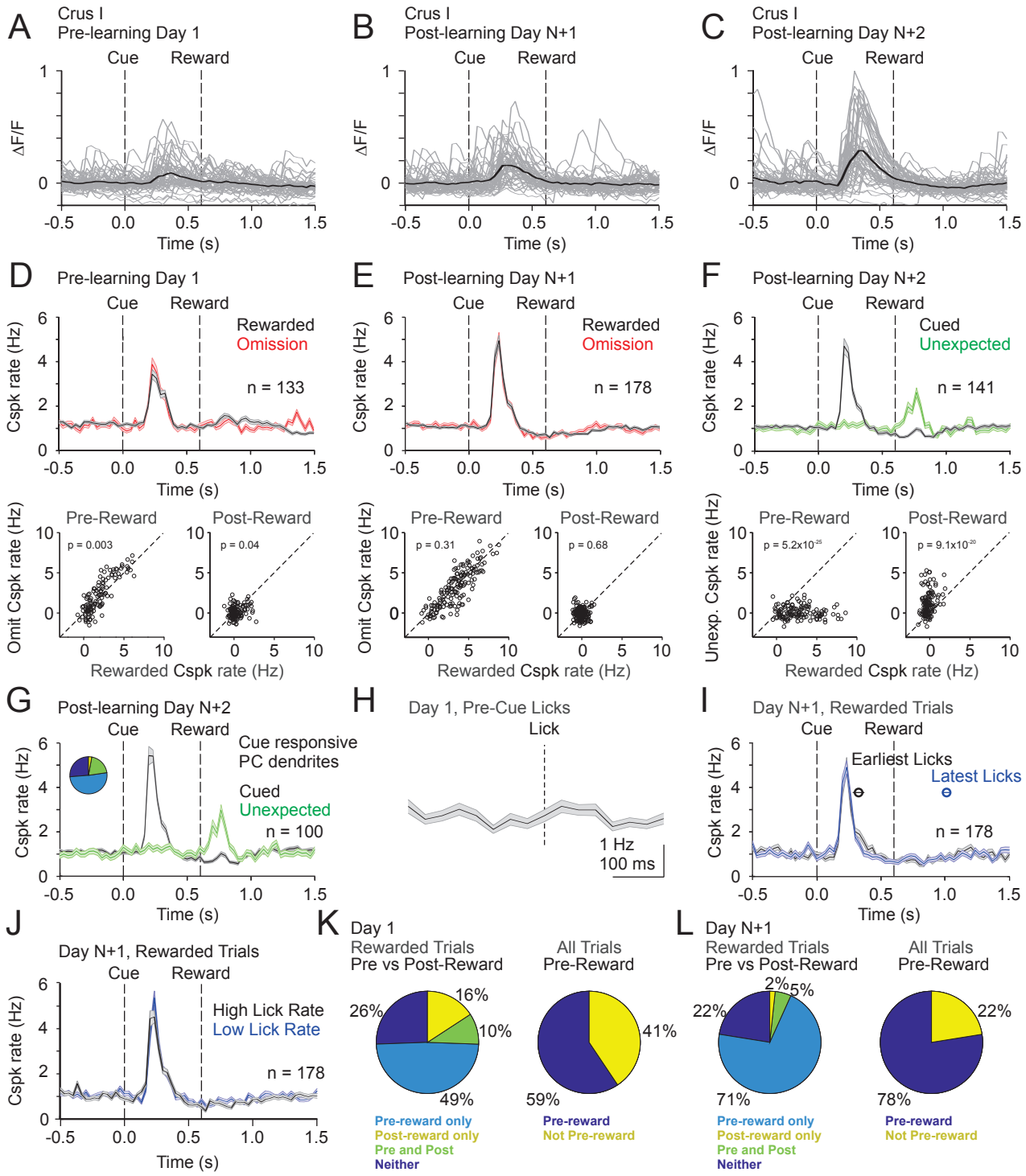
A
Crus I
Pre-learning Day 1
Cue
Reward
ΔF/F
Time (s)
B
Crus I
Post-learning Day N+1
C
Crus I
Post-learning Day N+2
D
Pre-learning Day 1
Rewarded
Omission
n = 133
Cspk rate (Hz)
E
Post-learning Day N+1
n = 178
F
Post-learning Day N+2
Cued
Unexpected
n = 141
Pre-Reward
Post-Reward
p = 0.003
p = 0.04
p = 0.31
p = 0.68
p = 5.2x10^-25
p = 9.1x10^-20
Omit Cspk rate (Hz)
Unexp. Cspk rate (Hz)
Rewarded Cspk rate (Hz)
G
Post-learning Day N+2
Cue responsive
PC dendrites
Cued
Unexpected
n = 100
H
Day 1, Pre-Cue Licks
Lick
1 Hz
100 ms
I
Day N+1, Rewarded Trials
Earliest Licks
Latest Licks
n = 178
J
Day N+1, Rewarded Trials
High Lick Rate
Low Lick Rate
n = 178
K
Day 1
Rewarded Trials
Pre vs Post-Reward
All Trials
Pre-Reward
26%
16%
10%
49%
41%
59%
Pre-reward only
Post-reward only
Pre and Post
Neither
Pre-reward
Not Pre-reward
L
Day N+1
Rewarded Trials
Pre vs Post-Reward
All Trials
Pre-Reward
22%
2%
5%
71%
22%
78%
Pre-reward only
Post-reward only
Pre and Post
Neither
Pre-reward
Not Pre-reward

Figure 5

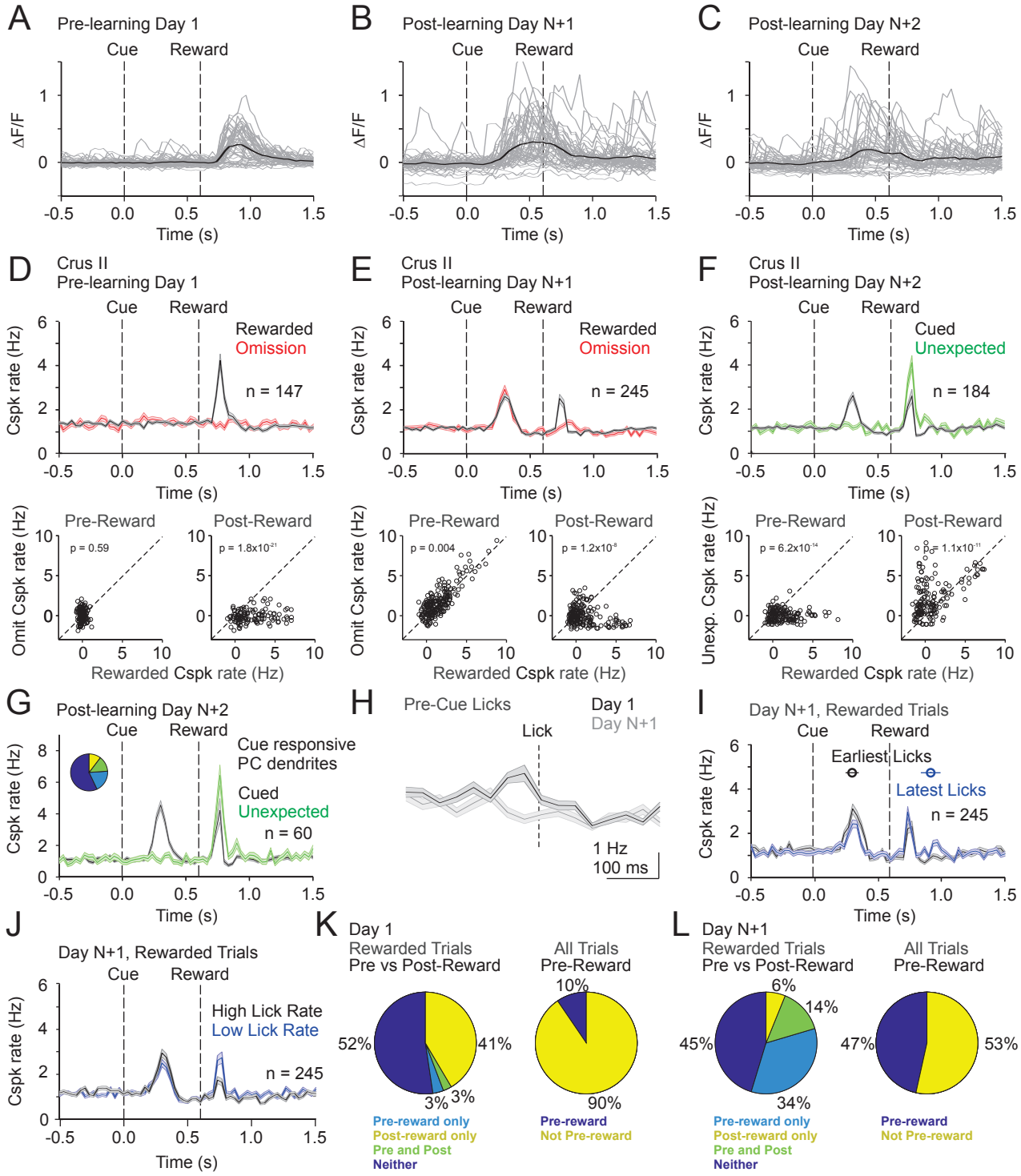
A
Pre-learning Day 1
Cue
Reward
ΔF/F
Time (s)
B
Post-learning Day N+1
C
Post-learning Day N+2
D
Crus II
Pre-learning Day 1
Rewarded
Omission
n = 147
Cspk rate (Hz)
E
Crus II
Post-learning Day N+1
n = 245
F
Crus II
Post-learning Day N+2
Cued
Unexpected
n = 184
Pre-Reward
Post-Reward
p = 0.59
p = 1.8x10-21
p = 0.004
p = 1.2x10-8
p = 6.2x10-14
p = 1.1x10-11
Omit Cspk rate (Hz)
Unexp. Cspk rate (Hz)
Rewarded Cspk rate (Hz)
G
Post-learning Day N+2
Cue responsive
PC dendrites
Cued
Unexpected
n = 60
H
Pre-Cue Licks
Day 1
Day N+1
Lick
1 Hz
100 ms
I
Day N+1, Rewarded Trials
Earliest Licks
Latest Licks
n = 245
J
Day N+1, Rewarded Trials
High Lick Rate
Low Lick Rate
n = 245
K
Day 1
Rewarded Trials
Pre vs Post-Reward
All Trials
Pre-Reward
52%
41%
3%
3%
10%
90%
Pre-reward only
Post-reward only
Pre and Post
Neither
Pre-reward
Not Pre-reward
L
Day N+1
Rewarded Trials
Pre vs Post-Reward
All Trials
Pre-Reward
6%
14%
45%
34%
47%
53%
Pre-reward only
Post-reward only
Pre and Post
Neither
Pre-reward
Not Pre-reward

Figure 6

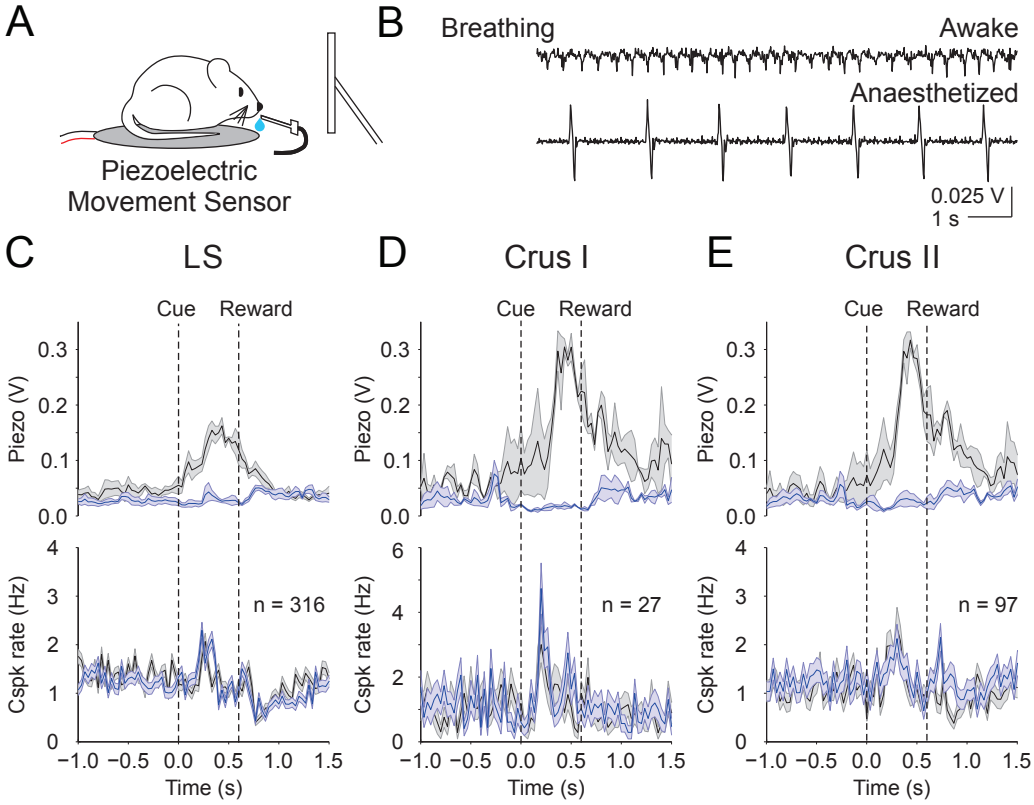
A
Piezoelectric
Movement Sensor
B
Breathing
Awake
Anaesthetized
0.025 V
1 s
C
LS
D
Crus I
E
Crus II
Cue
Reward
Piezo (V)
Cspk rate (Hz)
n = 316
n = 27
n = 97
Time (s)

Figure 7

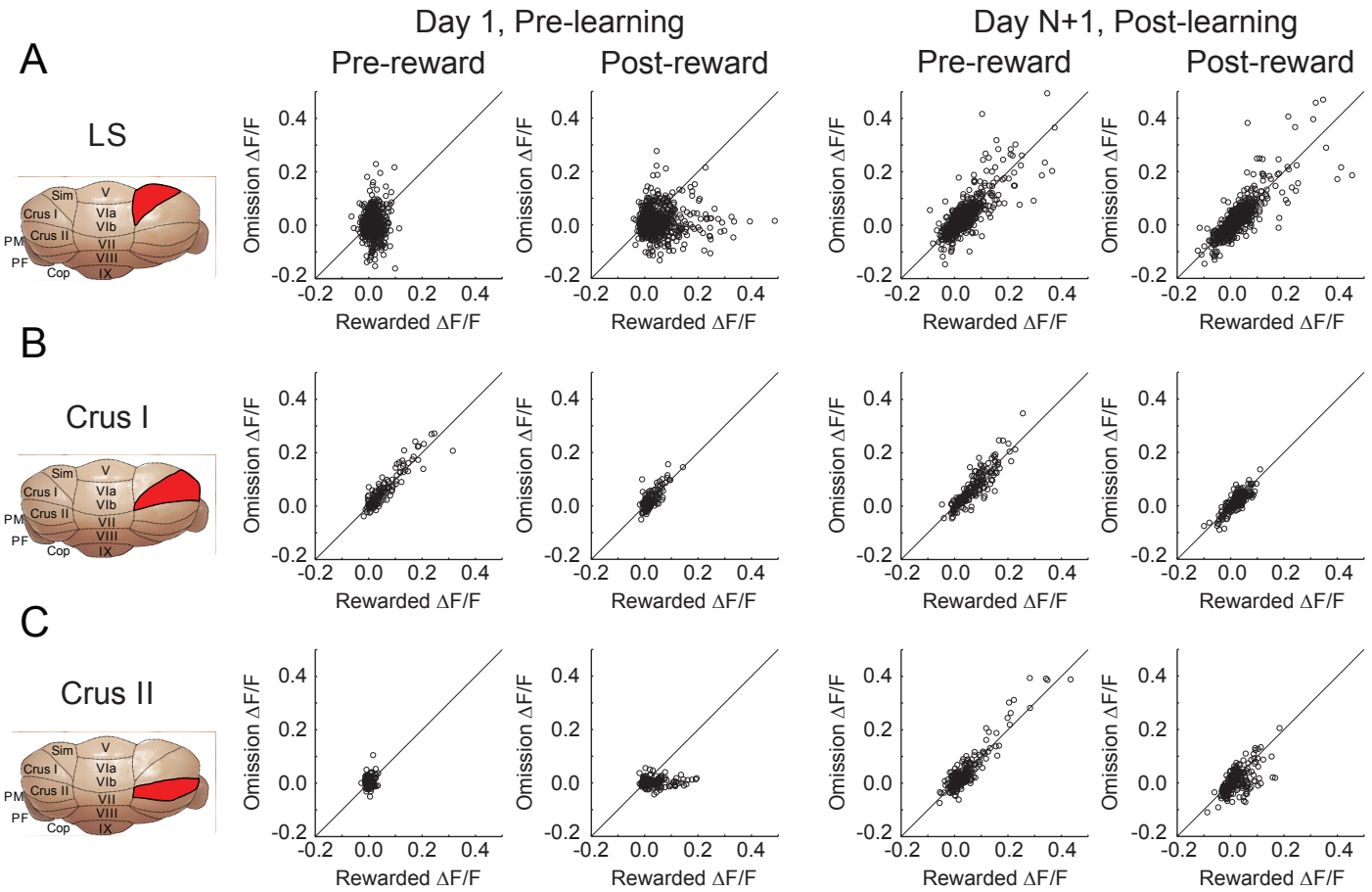

Fig. 3 - Figure Supplement 1

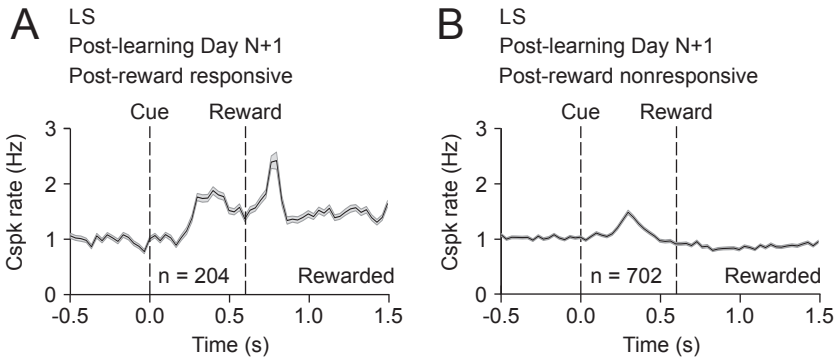

Fig. 3 - Figure Supplement 2

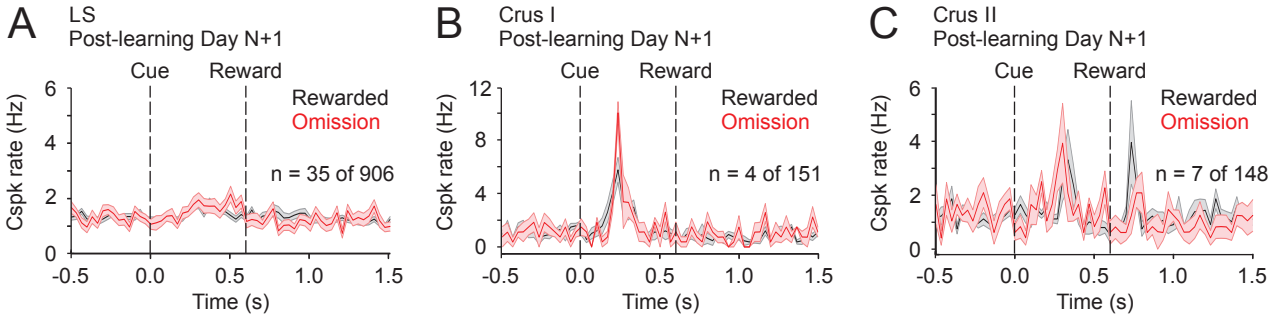

Fig. 3 - Figure Supplement 3